



Article

## Operation Conditions Investigation of An Adsorption Desalination / Cooling System Driven by Solar Energy

Mohamed Ghazy<sup>1,\*</sup>, Eslam Ibrahim<sup>2</sup>, A. S. A. Mohamed<sup>1,3</sup>, Ahmed Askalany<sup>1</sup>

<sup>1</sup>Mechanical Department, Faculty of Technology and Education, Sohag University, Sohag 82524, Egypt

<sup>2</sup>Physics Department, Faculty of Science, Sohag University, 82524-Sohag, Egypt

<sup>3</sup>High Institute for Engineering and Technology, Sohag, Egypt

\*Corresponding author: [ghazy2100@yahoo.com](mailto:ghazy2100@yahoo.com) Tel.:+201065652916

### Article info:

Citation: Ghazy, Mohamed, Ibrahim Eslam, Mohamed, A.S.A., & Askalany, Ahmed. A. (2022). Operation Conditions Investigation of An Adsorption Desalination/ Cooling System Driven by Solar Energy. *Sohag Journal of junior Scientific Researchers*, 2(2), 22 - 36.

<https://doi.org/10.21608/sjyr.2022.227426>

Received: 20/01/2022

Accepted: 21/02/2022

Published: 28/03/2022

Publisher's Note: SJYR stays neutral with regard to jurisdictional claims in published maps and institutional affiliations.

### Abstract

The main objectives of this research are directly related to the use of economic solutions to solve the problem of freshwater scarcity under Egypt's vision 2030. Adsorption desalination systems are an alternative technology to traditional water desalination systems. Adsorption desalination systems are characterized by the possibility of operating using a solar collector, which contributes to saving electricity and the possibility of applying it in remote areas. Also, desalination systems use environmentally friendly materials, limiting global warming and environmental pollution. Therefore, this work presents a study of the optimal operating conditions for an adsorption desalination system driven by solar energy in the climate of Sohag city-Egypt. The system uses one of the most efficient water vapor-absorbing adsorbents called MOF-27Ni. Optimum operating conditions include investigation of heating and cooling temperatures, flow rates, and operating time. It also includes a comparison between theoretical and practical results to verify the validity of the results. The results showed that the highest performance achieved 5 (m<sup>3</sup>/ton-day) specific daily water productions (SDWP) and 0.23 coefficient of performance (COP).

### Keywords

Adsorption, Desalination, Cooling, Solar energy, Renewable energy

## Nomenclature

| Symbol          | Description                                     | Unit    |
|-----------------|---|---------|
| $C_{p_{al}}$    | Aluminum specific heat                          | J/kg.K  |
| $C_{p_{ch}}$    | Chilled water specific heat                     | J/kg.K  |
| $C_{p_{cu}}$    | Copper specific heat                            | kg/s    |
| $C_{p_{sg}}$    | Silica gel specific heat                        | J/kg.K  |
| $C_{p_v}$       | Water specific heat vapor phase                 | J/kg.K  |
| $C_{p_w}$       | Water specific heat liquid phase                | J/kg.K  |
| $\dot{m}_{chw}$ | Chilled water flow rate                         | kg/s    |
| $\dot{m}_{cw}$  | Cooling water flow rate to adsorber             | kg/s    |
| $\dot{m}_{hw}$  | Heating water flow rate to adsorber             | kg      |
| $M_{al}$        | Bed heat exchanger fin weight(Al)               | kg      |
| $M_{bed,iron}$  | Bed heat exchanger cover weight(iron)           | kg      |
| $M_{con,cu}$    | Condenser heat exchanger tube weight(Cu)        | kg      |
| $M_{cu}$        | Bed heat exchanger tube weight(Cu)              | W/K     |
| $M_{eva}$       | Evaporator heat exchanger tube weight(Cu)       | kg      |
| $M_{sg}$        | Weight of silica gel in each bed                | kg      |
| $M_{w,eva}$     | Liquid water in side evaporator initially       | kg      |
| $T_{ch,in}$     | Chilled water inlet temperature                 | °C      |
| $T_{cw}$        | Cooling source temperature                      | °C      |
| $t_{cycle}$     | Cycle time                                      | s       |
| $T_{hw}$        | Heating source temperature                      | °C      |
| $UA_{bed,S}$    | Overall heat transfer coefficient of bed        | W/K     |
| $UA_{con}$      | Overall heat transfer coefficient of condenser  | W/K     |
| $UA_{eva}$      | Overall heat transfer coefficient of evaporator | W/K     |
| $R$             | Universal gas constant                          | J/mol.K |

## 1. Introduction

The global ambition for sustainable development is hampered by rapid social and economic development and continued population growth. This has led to the emergence of many challenges, most notably the lack of fresh water and the increased demand for energy consumption (IEA 2021). Worse, the lack of freshwater sources has increased the demand for industrial desalination systems driven by traditional energy sources such as fossil fuels. (Zervos, 2021) Therefore, researchers have focused on using renewable energy sources in all sectors, especially water desalination. (Chauhan et al., 2021) Adsorption technology is an outstanding candidate for desalination, cooling, and energy storage. It can efficiently and effectively address the relationship between energy and the environment efficiently and effectively because it can be powered by solar energy, geothermal heat, or low-grade heat sources. It does not include moving parts such as pumps or compressors. (Askalany et al., 2022) However, this technology is still of limited use compared to conventional systems due to lower performance in terms of specific cooling power (SCP), coefficient of performance (COP), and desalinated water yield. Therefore, many studies were conducted to improve the overall system performance, such as the design development and improvement of adsorbents materials properties.

The design development aims to improve the heat transfer process, especially between the adsorbent material and the heating/cooling fluid in the adsorption chamber, which reduces the

energy consumed and increases the performance factor. For this purpose, many heat exchangers have been investigated, such as finned-tube heat exchangers. (Alsaman et al., 2017), wire fin heat exchangers. (Saleh et al., 2020), a flat-plate heat exchanger. (Mohammed et al., 2017), a modular heat exchanger. (Mohammed et al., 2018), etc.

Also, improving the adsorption properties aims to absorb an immense amount of water vapor and thus increases the desalinated water yield and specific cooling capacity. The improvement of adsorptive materials includes either enhancing the conventional material's adsorption properties such as Silica-gel (Mohammed et al., 2019), zeolite (Rocky et al., 2021), copper sulfate (Ali et al., 2018) and activated carbon (Ghazy et al., 2021, Ahmed Askalany et al. 2016) or investigation of new/advanced materials such as organic metal frameworks (MOFs). MOFs offer competitive advantages in larger pore size and high surface area that exceed  $6000 \text{ m}^2/\text{g}$  [18,19], allowing for a large adsorption ratio, which has led to their widespread use over the past years. In this context, (Youssef et al., 2017) theoretically and experimentally verified the performance parameters of CPO-27Ni for an open-loop adsorption desalination system (condenser and evaporator not connected) driven by electric power. The results showed that the performance improved as the evaporator temperature increased and the condenser temperature decreased. The best results achieved a desalinated water production rate of 22 ton/day at a temperature of  $5^\circ\text{C}$  condenser,  $30^\circ\text{C}$  evaporator, and  $95^\circ\text{C}$  heating tank. (Al-Dadah et al., 2020) experimentally tested three MOF materials (aluminum fumarate, CPO-27(Ni), and MIL-100(Fe)) for the adsorption desalination, cooling, and thermal storage applications driven by electric power. It was found that the best results for desalination were  $19 \text{ m}^3/\text{ton-day}$  MIL-100(Fe),  $13 \text{ m}^3/\text{ton-day}$  aluminum fumarate, and  $10 \text{ ton/day}$  CPO-27(Ni). For cooling applications, MIL-100 (Fe) showed  $226 \text{ W/kg}$ , while aluminum fumarate produced  $136 \text{ W/kg}$  of SCP. The energy storage density was  $1200 \text{ Wh/kg}$  of MIL-100 (Fe) for thermal storage.

Table 1. Summary of the performance of MOFs used adsorption applications

| Ref.                        | MOF Adsorbent                 | Cold water           | Hot water            | Chilled water      | Time Half-cycle | CO <sub>P</sub> | SCP                    | SDW P<br>m <sup>3</sup> /ton / day | Application          |
|-----------------------------|-------------------------------|----------------------|----------------------|--------------------|-----------------|-----------------|------------------------|------------------------------------|----------------------|
| (Youssef et al. 2017)       | CPO-27Ni                      | $5^\circ\text{C}$    | $95^\circ\text{C}$   | $40^\circ\text{C}$ | 10 min          | NA              | $200 \text{ w/Kg}$     | 22.8                               | Desalination         |
| (Gediz Ilis 2017)           | NH <sub>2</sub> -MIL-125 (Ti) | $40.5^\circ\text{C}$ | $77.5^\circ\text{C}$ | $2^\circ\text{C}$  | 33000 s         | 0.87            | $7.66 \text{ kJ/Kg}$   | -                                  | Heat pump            |
| (Elsayed et al. 2019)       | MIL-101(Cr)                   | $30^\circ\text{C}$   | $90^\circ\text{C}$   | $10^\circ\text{C}$ | 500s            | 0.35            | $168-248 \text{ W/Kg}$ | -                                  | Desalination Cooling |
| (Han and Chakraborty 2020a) | UiO-66 (Zr)                   | $30^\circ\text{C}$   | $60^\circ\text{C}$   | $30^\circ\text{C}$ | 700 S           | 0.12            | $0.016 \text{ kW/Kg}$  | 24.9                               | Desalination         |
|                             | N-UiO-66 (Zr)                 | $30^\circ\text{C}$   | $60^\circ\text{C}$   | $30^\circ\text{C}$ | 300 S           | 0.4             | $0.25 \text{ kW/Kg}$   | 37.6                               | Heat pump cooling    |

|                             |                    |      |       |            |           |          |               |           |                              |
|-----------------------------|--------------------|------|-------|------------|-----------|----------|---------------|-----------|------------------------------|
| (Han and Chakraborty 2020b) | OH-UiO-66 (Zr)     | 30°C | 60 °C | 30°C       | 200 S     | 0.2<br>1 | 0.26<br>kW/Kg | 42        |                              |
|                             | NH2-UiO-66 (Zr)    | 30°C | 60 °C | 30°C       | 500 S     | 0.6<br>4 | 0.61<br>kW/Kg | 30.0      |                              |
|                             | MOF-801 (Zr)       | 30°C | 80°C  | 14.8°<br>C | 1000S     | 0.4<br>7 | 0.54<br>kW/Kg | -         | Desali-<br>nation<br>Cooling |
| (Elsayed et al. 2020)       | MIL-100(Fe)        | 30°C | 95°C  | 15°C       | 45<br>min | NA       | 226<br>W/Kg   | 19        | Desal-<br>ination            |
|                             | Aluminium fumarate | 30°C | 90°C  | 15°C       | 45<br>min | NA       | 136<br>W/Kg   | 13<br>day | Desal-<br>ination            |

(Elsayed et al., 2017a) compared the performance of the AD cycle using CPO-27(Ni), MIL-101(Cr), and aluminum fumarate. It was shown that the CPO-27(Ni) could deliver daily freshwater of about 4.3 m<sup>3</sup>/ton at 5°C evaporator temperature. 6 m<sup>3</sup>/ton and 11 m<sup>3</sup>/ton of potable water were produced using aluminum fumarate and MIL-101(Cr), respectively, at an evaporator temperature of 20 °C. The most famous organic framework materials used in adsorption desalination applications were summarized with their operating conditions in Table 1.

Despite the studies that were conducted on MOFs, especially COP-27Ni, it was found that there is a research gap that was not covered, which is the performance examination using the solar collector under actual climatic conditions. This is due to the lack of solar radiation in most areas. Therefore, the authors found that Egypt has an abundance of solar radiation and provides ideal climatic conditions for testing adsorption desalination systems; especially, it can be adopted as an alternative desalination system to conventional desalination systems. Hence, this work presents an experimental and theoretical investigation of the performance of an adsorption desalination system driven by solar energy. The desalination system uses COP-27Ni as an adsorbent and water as an adsorbate. The study includes examining the optimal operating conditions in terms of coefficient of performance, specific cooling power, and water desalinated production.

## 2- Experimental work

### 2.1 System description

The desalination/adsorption cooling system consists of four essential components; Two absorption beds, a condenser, and an evaporator. The adsorption bed is a sealed stainless steel cylinder with a three-layer heat exchanger of a finned tube filled with 1.8 kg of Sibo adsorbent. CPO-27Ni used in this work is a MOF adsorbent manufactured commercially by Johnson Matthey, and its physical properties are listed in Table 2 (Youssef et al., 2017; Elsayed et al., 2017a; Elsayed et al. 2017b). The function of the adsorption bed is to maintain the vacuum pressure in the circuit, where the adsorbent material draws and adsorption of water vapor from the evaporator at low temperature and then expels it back to the condenser when heating at high temperatures. It is worth noting that when one of the adsorption beds is in the turbine mode, the other is in heating mode to ensure the continuation of the cycle, and this reason is the pres-

ence of two adsorption beds in the system. The condenser is a stainless steel vessel containing a condensing coil that uses water as a coolant. The function of the condenser is to receive water vapor from the adsorption beds and condense it to obtain desalinated water. The condenser only opens with the adsorption bed in the heating (adsorption) mode. The evaporator is also a stainless steel vessel containing on helical coil a water-driven. The function of the evaporator is to convert saltwater into water vapor. The evaporator receives the sea and then turns into water vapor by low pressure, and then it is sent to the cooled adsorption bed (in adsorption mode).

## 2.2 Experimental procedure

This part illustrates the steps of operating and testing the adsorption desalination system, as shown in Figure 2.

- 1- Initially, the system is vacuumed by opening the vapor valves of the components (adsorption bed, condenser, and evaporator) to the vacuum pump until the pressure reaches 0.01 kPa; all valves are closed vacuum pump is isolated.
- 2- The evaporator is fed with salt water until the chilled water coil is immersed. The evaporation of water is observed until the evaporator space is saturated with water vapor due to the vacuum pressure inside it.
- 3- The desorption phase (heating the adsorption bed 1) is activated by opening the water valves of bed 1 to the hot water tank and the solar collector, called the pre-heating process.
- 4- The adsorption phase (cooling the adsorption bed 2) is activated by opening the water valves of bed 2 and the condenser to the cold water tank, called the pre-cooling process.
- 5- When the pressure inside the adsorption bed 2 drops below the evaporator, the steam valves are opened between the evaporator and the adsorption bed 2. The process is called adsorption and allows CPO-27Ni material to adsorb the water vapor coming from the evaporator until saturation.
- 6- When the pressure inside the adsorption bed 1 increases higher than the condenser's pressure, the vapor valves are opened between the condenser and the adsorption bed 1. The process is called desorption and allows the CPO-27Ni material to desorb the water vapor and flow into the condenser and then condense it to get desalinated water.
- 7- The stages are reversed so that the adsorption phase is activated in the adsorption bed 1, as well as the desorption phase is activated in the adsorption bed 2 to obtain a continuous cycle and stable performance.



Figure 1. Photo of experimental adsorption desalination system

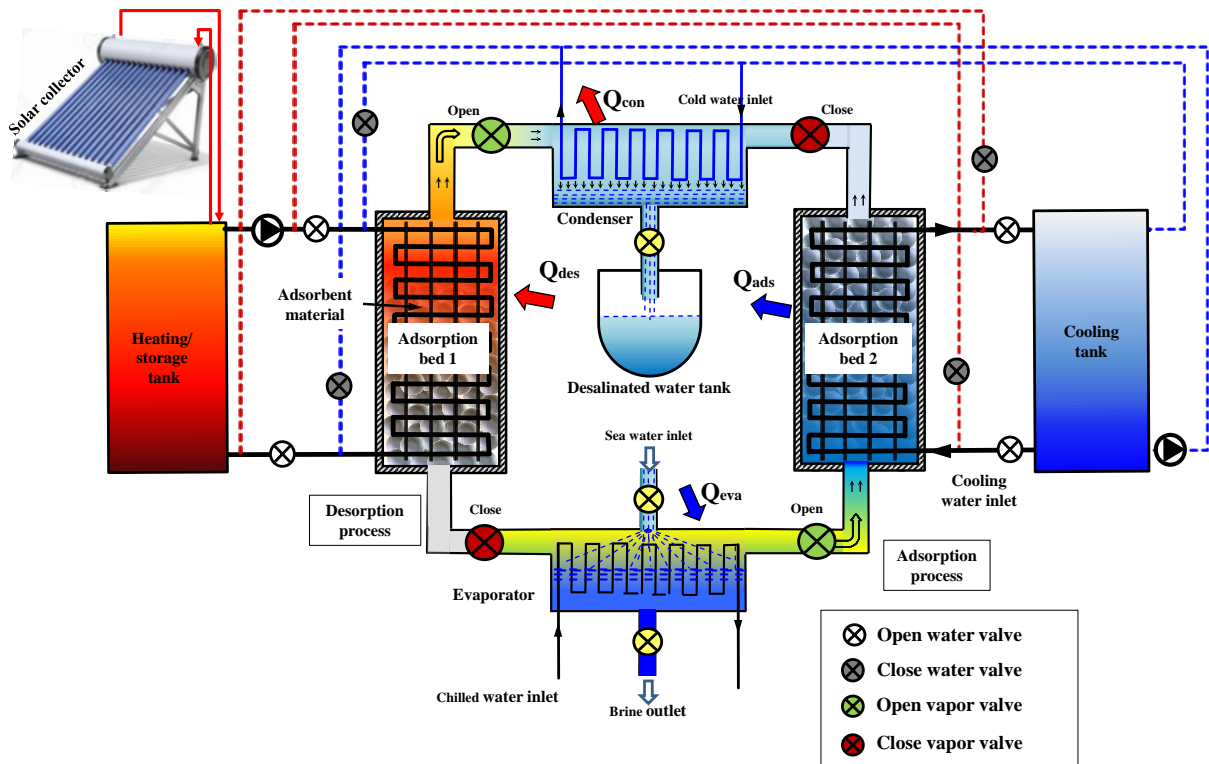


Figure 2. Schematic diagram of details of adsorption desalination system.

### 3- Mathematical Model

#### 3.1 Energy balances

In the clause-parameter mathematical technique, the adsorbent material, water vapor, and metal in one adsorption bed are assumed to have an equal temperature. Hence, the following equations describe the energy balance of adsorption beds.

$$\frac{dT_{ads}}{dt} \left[ (M_{ac} C_{p,ac}) + (M_{cu} C_{p,cu}) + \left( M_{ac} C_{p,Mixture} \frac{dw_{ads}}{dt} \right) \right] = \left[ \left( qH_{st} M_{ac} \frac{dw_{ads}}{dt} \right) - m^{\bullet}_w C_{p,cwa} (T_{cwa,out} - T_{cwa,in}) \right] \quad (1)$$

Cooling fluid outlet temperature  $T_{cwa,out}$  is calculated by Eq. 2.

$$T_{cwa,out} = T_{ads} + (T_{cwa,in} - T_{ads}) \exp \left( \frac{-U_{ads} A_{ads}}{m^{\bullet}_{wa} c_{p,wa}} \right) \quad (2)$$

The desorption energy balance is described by:

$$\frac{dT_{des}}{dt} \left[ (M_{ac} C_{p,ac}) + (M_{cu} C_{p,wd,cu}) + \left( M_{ac} C_v \frac{dw_{des}}{dt} \right) \right] = \left[ \left( qH_{st} M_{ac} \frac{dw_{des}}{dt} \right) - m^{\bullet}_{hw,d} C_{p,hw,d} (T_{hw,d,out} - T_{hw,d,in}) \right] \quad (3)$$

Eq. 4 describes heating fluid outlet temperature  $T_{hwd,out}$ .



$$T_{hwd,out} = T_{des} + (T_{hwd,in} - T_{des}) \exp\left(\frac{-U_{des} A_{des}}{m_{wd} \cdot c_{p,wd}}\right) \quad (4)$$

Condenser energy equation can be described by:

$$\frac{dT_{cond}}{dt} (M_{cu,cond} C_{p,cu} + M_v C_v) = \left(-M_{ac} h_{fg} \frac{dw_{des}}{dt}\right) + m_{cwc} \cdot C_{p,w} (T_{cwc,in} - T_{cwc,out}) \quad (4)$$

Where  $M_{cu,cond}$ , and  $M_v$  are the mass of the copper tubes and water vapor in the condenser, respectively. Condenser outlet water temperature is calculated using the log mean temperature difference (LMTD) approach as:

$$T_{cwc,out} = T_{cond} + (T_{cwc,in} - T_{cond}) \exp\left(\frac{-U_{cond} A_{cond}}{m_{cwc} \cdot C_{p,cw}}\right) \quad (5)$$

Energy equation that has been utilized to express inlet and outlet heats of the evaporator is as follows:

$$\frac{dT_{eva}}{dt} (M_{cu,eva} C_{p,cu,eva} + M_v C_v) = \left(-h_{fg} M_{ac} \frac{dw_{ads}}{dt}\right) + m_{chill} \cdot C_{p,chill} (T_{chill,in} - T_{chill,out}) \quad (6)$$

Evaporator outlet water temperature is calculated using the LMTD approach as:

$$T_{chill,out} = T_{eva} + (T_{chill,in} - T_{eva}) \exp\left(\frac{-U_{eva} A_{eva}}{m_{chill} \cdot C_{p,chill}}\right)$$

(7)

#### 4.5 Mass balance

$$\frac{dC_{eva}}{dt} = -M_{ac} \frac{dC_{des}}{dt} - M_{ac} \frac{dC_{ads}}{dt} \quad (8)$$

Where,  $M_{ac}$  is the mass of adsorbents packed in each of the two adsorbent beds and  $C_{eva}$  is the vapor mass.

#### 4.6 System performance

The main parameters that determine adsorption desalination performance are SDWP and COP, which can be calculated from the following equations:

$$Q_{chill}^{cycle} = \int_0^{t_{cycle}} \left\{ (m_{cw} \cdot c_{p,w})_{chill} (T_{chill,in} - T_{chill,out}) \right\} dt \quad (9)$$

$$Q_{des}^{cycle} = \int_0^{t_{cycle}} \left\{ (m_{hw} \cdot c_{p,w})_{des} (T_{hw,in} - T_{hw,out}) \right\} dt \quad (10)$$



$$COP = \frac{Q_{chill}^{cycle}}{Q_{des}^{cycle}} \tag{12}$$

Where  $M_{ac}$  is the adsorbent weight.

$$SDWP = \int_0^{t_{cycle}} \frac{(m_{cw} \cdot c_{p,w})(T_{cw,out} - T_{cw,in}) \tau dt}{h_{fg} M_{ac}} \tag{13}$$

#### 4- Result and discussion

##### 4.1 operation conditions

Figure 3 shows the effect of cycle time on SDWP and COP at a desorption temperature of 95°C, a cooling water temperature of 30 °C, and a water flow rate of 6 L/min. It can be seen that SDWP improves with increasing cycle time up to 380-400 seconds and then decreases with increasing cycle time. On the other hand, COP increases when cycle time increases. Therefore, it can be concluded that the optimal cycle time can be set at 400 s.

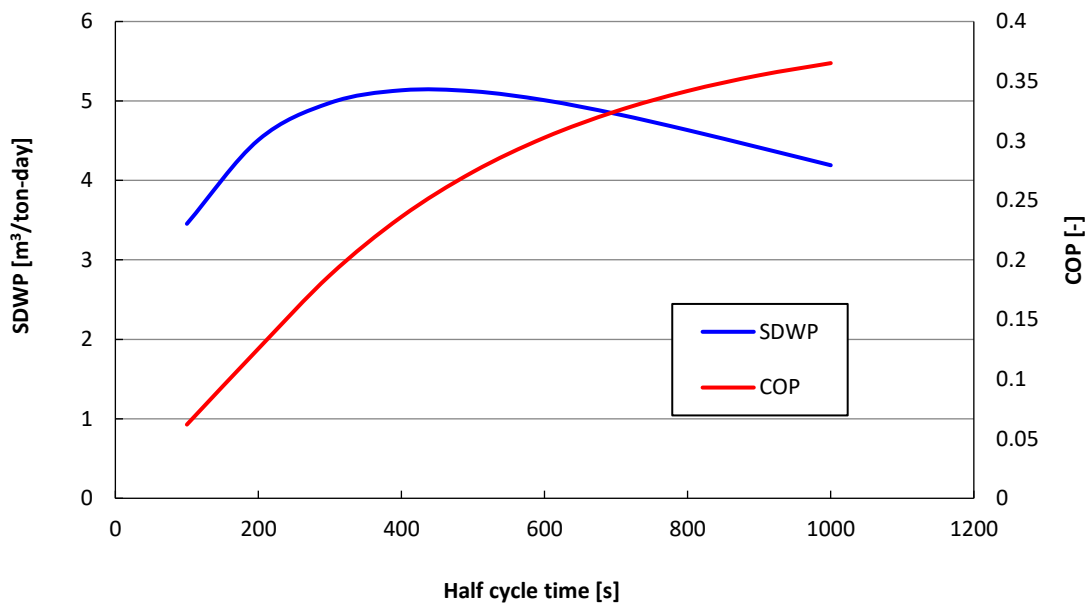


Figure 3: Effect of cycle time on SDWP and COP.

Figure 4 illustrates the effect of hot water temperature (desorption temperature) on SDWP and COP at a 400 s cycle time, a cooling water temperature of 30 °C, and a water flow rate of 6 L/min. It can be observed that both SDWP and COP are enhanced by increasing the hot water temperature. It indicates that the adsorption desalination system can be powered by a flat plate and concentrated solar collector. The permissible hot water temperature range can start from 75°C for the flat collector to 135°C for the concentrated solar collector.

Figure 5 shows the effect of cooling water temperature (adsorption temperature) on SDWP and COP at a 400 s cycle time, a hot water temperature of 95 °C, and a water flow rate of 6 L/min. It can be noted that both SDWP and COP decrease with increasing the cooling water tempera-

ture. The permissible cooling water temperatures are filled in the range of 10°C to 45°C, where the maximum result achieved 14 m<sup>3</sup>/ton-day of SDWP, and .4 COP at 10°C, and the lowest and results were about 1.8 m<sup>3</sup>/tine-day of SDWP and 0.07 at 45°C COP for the flat collector to 135°C for the concentrated solar collector.

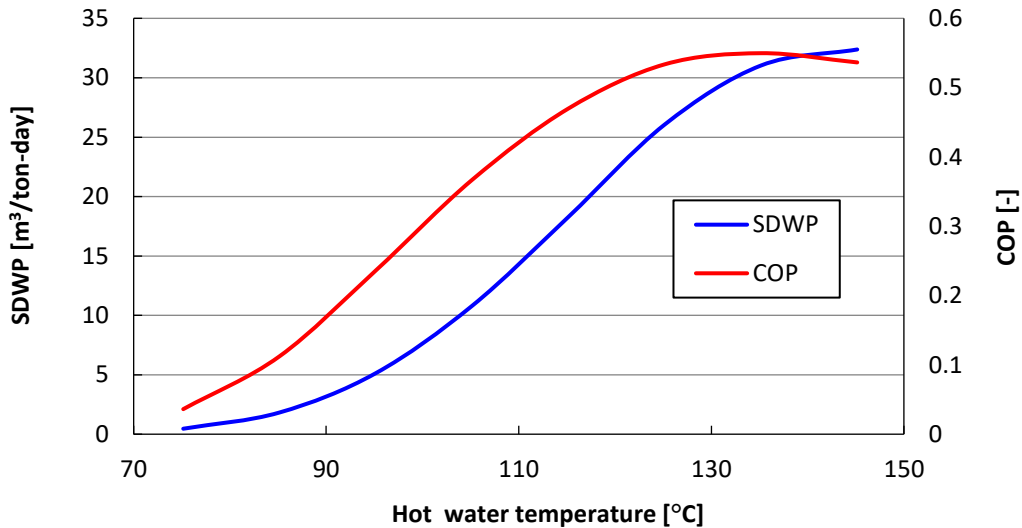


Figure 4: Effect of hot water temperature on SDWP and COP.

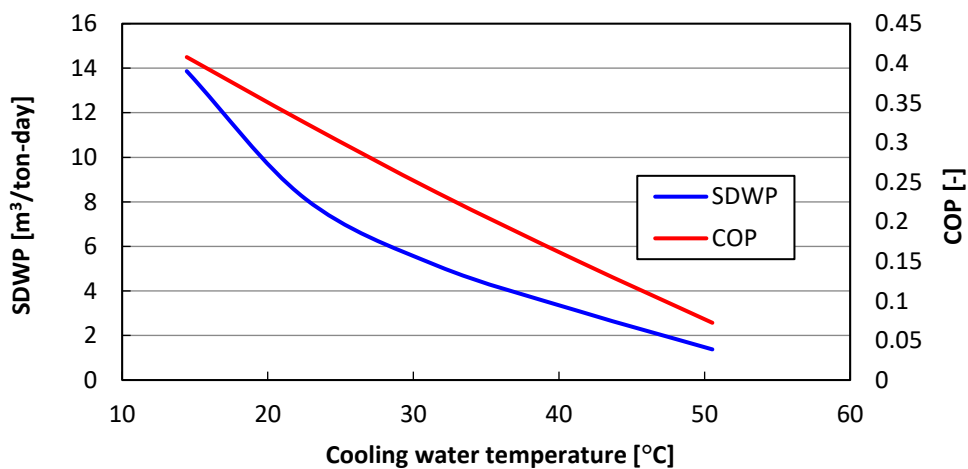


Figure 5: Effect of cooling water temperature on SDWP and COP.

Figure 6 depicts the influence of water flow rate on the performance parameters at a 400 s cycle time, a 95°C hot water temperature, and a 30°C cooling water temperature. It can be noted that both SDWP and COP increase significantly with increasing water flow rates until 6 L/min, then the increase slightly until 10 L/min. The slight increase of the performance parameters opposite the high flow rate increase indicates that the outcomes of the system will be less than the power consumed. So, the optimum flow rate should be at 6L/min.

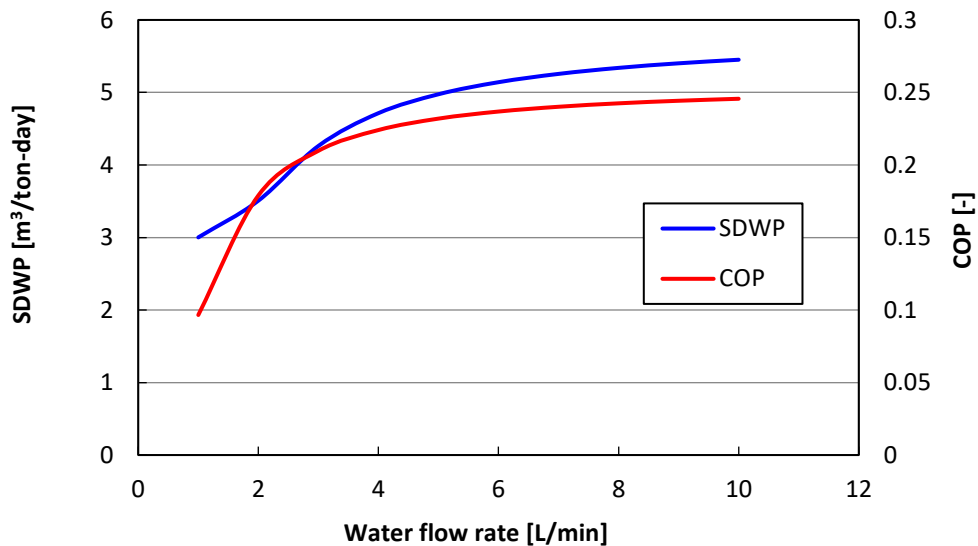


Figure 6. Effect of water flow rate on SDWP and COP

#### 4.2 Experimental results and validation

Figure 7 charts the solar radiation and solar collector temperature under the weather of Sohag City on 15th Jun. It can be noted that Sohag city has immense solar radiation reaching  $1000\text{W/m}^2$  at peak time, which positively affects solar collector temperature. So, the collector temperature ranged between  $80^\circ\text{C}$ -  $95^\circ\text{C}$ , driving the adsorption desalination system without an auxiliary heater. On the other hand, there is a harmony validation between the experimental and theoretical solar radiation results.

Figure 8 plots the experimental and theoretical temperature profile of the adsorption desalination system as a validation procedure. It can be noted that there is an agreement between the theoretical and experimental work, especially after the first half cycle, because the cooling and heating water temperatures are more stable with the system components.

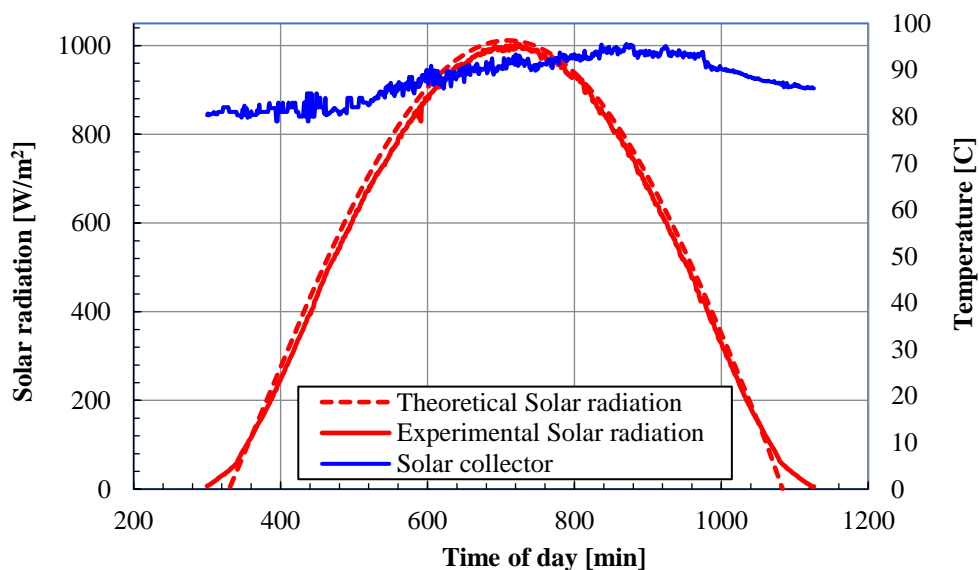


Figure 7. Temperature and solar radiation profile of solar collector.

Figure 9 outlines the validation of performance parameters of the adsorption desalination system. It can be seen that the agreement between the theoretical and experimental work is up to 95%. The maximum SDWP and COP reached 5 m<sup>3</sup>/ton-day and .23, respectively, at 95C hot water temperature.

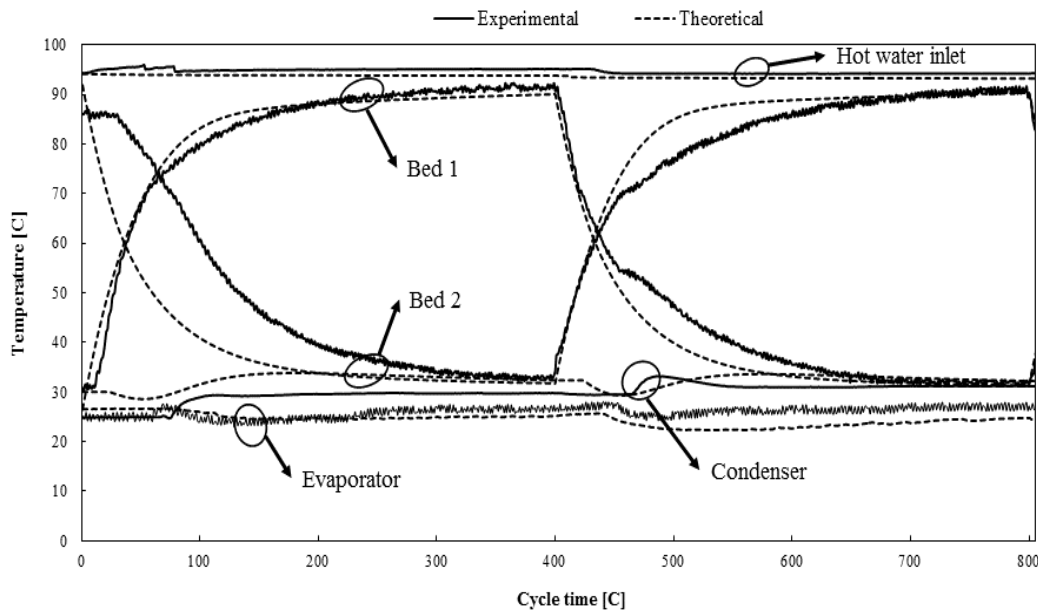


Figure 8. validation of adsorption desalination system's temperature profile.

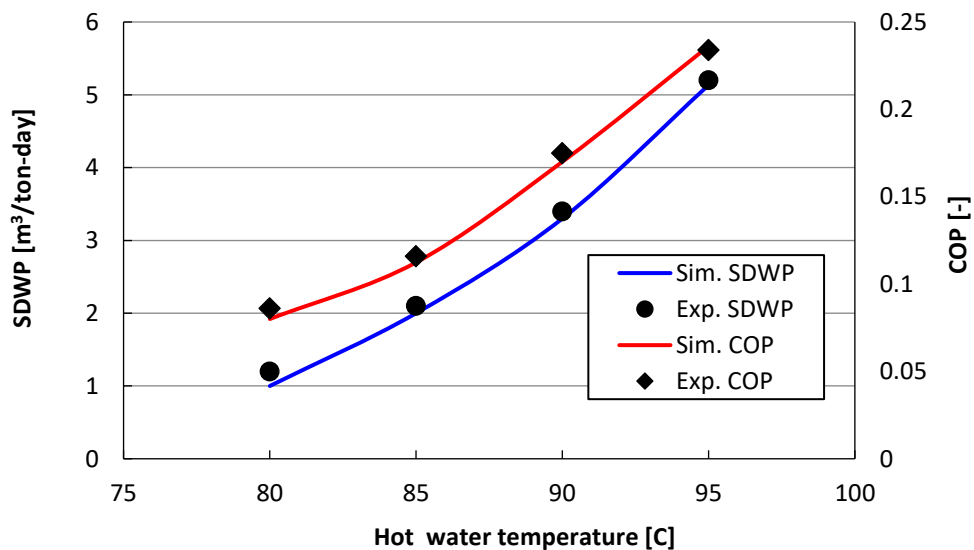


Figure 9. validation of adsorption desalination system's performance parameters.

### 5- Conclusion

This work is investigated the operation conditions of the adsorption desalination system power by a solar collector. The theoretical results are validated by experimental testing under weather conditions of Sohag city. The results showed a good agreement between the theoretical and experimental data up to 95%. The optimum conditions of the experimental investiga-

tion are evaluated as 400s half-cycle time, 6 L/min water flow rate, 30C cooling water temperature, and 95C heating water temperature. The adsorption desalination system produced 5 m<sup>3</sup>/ton-day with 0.23 COP at the optimum operating conditions.

## References

- Ahmed Askalany, Khairul Habib, M. Ghazy and Assadi, M.K. (2016) Adsorption cooling system employing activated carbon/hfc410a adsorption pair. *ARPN Journal of Engineering and Applied Sciences* 11.
- Al-Dadah, R., Mahmoud, S., Elsayed, E., Youssef, P. and Al-Mousawi, F. (2020) Metal-organic framework materials for adsorption heat pumps. *Energy* 190, 116356.
- Ali, E.S., Askalany, A.A., Harby, K., Diab, M.R. and Alsaman, A.S. (2018) Adsorption desalination-cooling system employing copper sulfate driven by low grade heat sources. *Applied Thermal Engineering* 136, 169-176.
- Alsaman, A.S., Askalany, A.A., Harby, K. and Ahmed, M.S. (2017) Performance evaluation of a solar-driven adsorption desalination-cooling system. *Energy* 128, 196-207.
- Askalany, A.A., Uddin, K., Saha, B.B., Sultan, M. and Santori, G. (2022) Water desalination by silica supported ionic liquid: Adsorption kinetics and system modeling. *Energy* 239, 122069.
- Chauhan, V.K., Shukla, S.K., Tirkey, J.V. and Singh Rathore, P.K. (2021) A comprehensive review of direct solar desalination techniques and its advancements. *Journal of Cleaner Production* 284, 124719.
- Elsayed, A., Elsayed, E., Al-Dadah, R., Mahmoud, S., Elshaer, A. and Kaialy, W. (2017b) Thermal energy storage using metal-organic framework materials. *Applied Energy* 186, 509-519.
- Elsayed, E., Al-Dadah, R., Mahmoud, S., Anderson, P. and Elsayed, A. (2019) Adsorption cooling system employing novel MIL-101(Cr)/CaCl<sub>2</sub> composites: Numerical study. *international journal of refrigeration* 107, 246-261.
- Elsayed, E., Al-Dadah, R., Mahmoud, S., Anderson, P. and Elsayed, A. (2020) Experimental testing of aluminium fumarate MOF for adsorption desalination. *Desalination* 475, 114170.
- Elsayed, E., Al-Dadah, R., Mahmoud, S., Anderson, P.A., Elsayed, A. and Youssef, P.G. (2017a) CPO-27(Ni), aluminium fumarate and MIL-101(Cr) MOF materials for adsorption water desalination. *Desalination* 406, 25-36.
- Gediz Ilis, G. (2017) Influence of new adsorbents with isotherm Type V on performance of an adsorption heat pump. *Energy* 119, 86-93.
- Ghazy, M., Askalany, A., Kamel, A., Khalil, K.M.S., Mohammed, R.H. and Saha, B.B. (2021) Performance enhancement of adsorption cooling cycle by pyrolysis of Maxsorb III activated carbon with ammonium carbonate. *international journal of refrigeration* 126, 210-221.
- Han, B. and Chakraborty, A. (2020a) Advanced cooling heat pump and desalination employing functional UiO-66 (Zr) metal-organic frameworks. *Energy conversion and management* 213.
- Han, B. and Chakraborty, A. (2020b) Adsorption characteristics of methyl-functional ligand MOF-801 and water systems: Adsorption chiller modelling and performances. *Applied Thermal Engineering* 175.
- IEA (2021) World Energy Outlook (IEA)

- 
- Mohammed, R.H., Mesalhy, O., Elsayed, M.L. and Chow, L.C. (2017) Novel compact bed design for adsorption cooling systems: Parametric numerical study. *international journal of refrigeration* 80, 238-251.
- Mohammed, R.H., Mesalhy, O., Elsayed, M.L. and Chow, L.C. (2018) Performance evaluation of a new modular packed bed for adsorption cooling systems. *Applied Thermal Engineering* 136, 293-300.
- Mohammed, R.H., Mesalhy, O., Elsayed, M.L. and Chow, L.C. (2019) Performance enhancement of adsorption beds with silica-gel particles packed in aluminum foams. *international journal of refrigeration* 104, 201-212.
- Rocky, K.A., Pal, A., Rupam, T.H., Nasruddin and Saha, B.B. (2021) Zeolite-graphene composite adsorbents for next generation adsorption heat pumps. *Microporous and mesoporous materials* 313, 110839.
- Saleh, M.M., Al-Dadah, R., Mahmoud, S., Elsayed, E. and El-Samni, O. (2020) Wire fin heat exchanger using aluminium fumarate for adsorption heat pumps. *Applied Thermal Engineering* 164, 114426.
- Youssef, P.G., Dakkama, H., Mahmoud, S.M. and Al-Dadah, R.K. (2017) Experimental investigation of adsorption water desalination/cooling system using CPO27-Ni MOF. *Desalination* 404, 192-199.
- Zervos, A. (2021) *Renewables 2021 Global Status Report*. Adib, R. (ed), REN21 202, <https://www.ren21.net/reports/global-status-report/>

## الملخص العربي

### فحص ظروف التشغيل لنظام تحلية / تبريد امتزاز يعمل بالطاقة الشمسية

محمد غازى\*<sup>1</sup>، اسلام ابراهيم<sup>2</sup>، احمد عسقلاني<sup>1</sup>، و احمد سعيد<sup>1,3</sup>

<sup>1</sup> قسم الميكانيكا - كلية التكنولوجيا والتعليم - جامعة سوهاج - سوهاج - مصر 82524

<sup>2</sup> قسم الفيزياء - كلية العلوم - جامعة سوهاج - سوهاج - مصر 82524

<sup>3</sup> المعهد العالي للهندسة والتكنولوجيا ، سوهاج ، مصر

\*المؤلف المسئول: [ghazy2100@yahoo.com](mailto:ghazy2100@yahoo.com)

ترتبط الأهداف الرئيسية لهذا البحث ارتباطًا مباشرًا باستخدام الحلول الاقتصادية لحل مشكلة ندرة المياه العذبة في ظل رؤية مصر 2030. أنظمة تحلية المياه بالامتزاز هي تقنية بديلة لأنظمة تحلية المياه التقليدية. تتميز أنظمة التحلية بالامتزاز بإمكانية التشغيل باستخدام مجمع شمسي مما يساهم في توفير الكهرباء وإمكانية تطبيقه في المناطق النائية. أيضا ، تستخدم أنظمة تحلية المياه بالامتزاز مواد صديقة للبيئة ، مما يحد من ظاهرة الاحتباس الحراري والتلوث البيئي. لذلك ، يقدم هذا العمل دراسة لظروف التشغيل المثلى لنظام تحلية بالامتصاص يعمل بالطاقة الشمسية في مناخ مدينة سوهاج - مصر. يستخدم النظام أحد أكثر المواد الماصة لبخار الماء كفاءة تسمى MOF-27Ni. تشمل ظروف التشغيل المثلى فحص درجات حرارة التدفئة والتبريد ومعدلات التدفق ووقت التشغيل. كما يتضمن مقارنة بين النتائج النظرية والعملية للتحقق من صحة النتائج. أظهرت النتائج أن أعلى أداء حقق 5 (م / 3 / طن / يوم) إنتاجات مائية محددة يومياً (SDWP) و 0.23 معامل أداء (COP).